Delft University of Technology

Stochastic Aerospace Systems Practicum
AE4304P

Symmetrical Aircraft Responses for a Rigid Aircraft in Symmetrical Atmospheric Turbulence Conditions

Authors:
Luc Kloosterman (4697006)

March 31, 2020

Contents

Introduction

Atmospheric turbulence is a stochastic air motion characterized by winds that vary in velocity and direction and cause a significant influence on aircraft motion and its trajectory. Severity of turbulence depends on the speed at which the wind velocity and direction changes. It can cause, if not accounted for, serious drift from the intended trajectory which is especially dangerous during take-off, approach and landing operations. Also, flying through turbulence causes extra loads and stresses on the airframe which should be taken into account when designing the aircraft. Besides these safety concerns, severe turbulence is also a concern for passenger comfort. Therefore, modelling turbulence is an essential aspect of designing an acceptable control system.

In this report, the symmetrical aircraft responses for a rigid Cessna Ce550 Citation II in cruise configuration subjected to symmetrical atmospheric turbulence will be analysed. The Power Spectral Density function of atmospheric turbulence is according to the model of Dryden. All calculations of aircraft responses to combined symmetric vertical and longitudinal turbulence are performed with the following parameters:

- $L_g = 150$ m
- $\sigma_{u_g} = 1$ m/s
- $\sigma_{w_g} = 1$ m/s

In the first section, a reduced model based on short-period assumptions will be derived and the stability of the complete and the reduced model will be analysed. Throughout this report all calculations will be executed on both aircraft models. After the stability analysis, a time-domain analyses will be executed by simulating the responses of the aircraft state variables and the load factor. In the third section, the analytical and experimental Power Spectral Density functions are calculated for the same states. At last, the variances of the states are calculated using the analytical power spectra, the impulse response function and the variance function from Matlab.

1 Stability Analysis

In this section, the stability analysis will be executed for the complete symmetric equations of motion, as well as a reduced version based on assumption applicable to the short period. The models are represented by a state space system which has the form shown in equation 1. First, the stability of the complete system will be analysed prior to designing a pitch damper to enforce a stable behavior. After this, the reduced aircraft model will be derived and a stability analysis will be done for this model.

$$\dot{X} = AX + BU \tag{1}$$

1.1 Uncontrolled Complete Aircraft Model

The state vector and the control input vector are defined respectively by equations 2 and 3. The inputs δ_e, w_1 and w_3 represent the elevator deflection, longitudinal turbulence and vertical turbulence respectively. The A and B matrices of the state space system are depicted by equations 4 and 5. Substituting the constants of the Cessna Ce550 Citation II gives the matrices depicted by equations 6 and 7. From the A matrix the eigenvalues can be calculated in order to analyse the stability. The eigenvalues are shown in table 1 and can be inspected visually in the pole-zero map of figure 1. From this it can be observed that the model has two eigenvalues which have a positive real part. Because of this it can be concluded that the model containing the complete symmetric equations of motions is unstable and needs an additional controller.

$$X = \begin{bmatrix} \hat{u} & \alpha & \theta & \frac{q\bar{c}}{V} & \hat{u}_g & \alpha_g & \alpha_g^* \end{bmatrix}^T \tag{2}$$

$$U = \begin{bmatrix} \delta_e & w_1 & w_3 \end{bmatrix}^T \tag{3}$$

$$A = \begin{bmatrix} x_u & x_\alpha & x_\theta & 0 & x_{u_g} & x_{a_g} & 0 \\ z_u & z_\alpha & z_\theta & z_q & z_{u_g} - z_{\dot{u}_g}\frac{V}{L_g}\frac{\bar{c}}{V} & z_{\alpha_g} & z_{\dot{\alpha}_g}\frac{\bar{c}}{V} \\ 0 & 0 & 0 & \frac{V}{\bar{c}} & 0 & 0 & 0 \\ m_u & M_\alpha & m_\theta & m_q & m_{u_g} - m_{\dot{u}_g}\frac{V}{L_g}\frac{\bar{c}}{V} & m_{\alpha_g} & m_{\dot{\alpha}_g}\frac{\bar{c}}{V} \\ 0 & 0 & 0 & 0 & -\frac{V}{L_g} & 0 & 0 \\ 0 & 0 & 0 & 0 & 0 & 0 & 1 \\ 0 & 0 & 0 & 0 & 0 & -\frac{V^2}{L_g^2} & -2\frac{V}{L_g} \end{bmatrix} \tag{4}$$

$$B = \begin{bmatrix} x_{\delta_e} & 0 & 0 \\ z_{\delta_e} & z_{\dot{u}_g}\frac{\bar{c}}{V}\sigma_{\hat{u}_g}\sqrt{\frac{2V}{l_g}} & z_{\dot{\alpha}_g}\frac{\bar{c}}{V}\sigma_{\alpha_g}\sqrt{\frac{3V}{l_g}} \\ 0 & 0 & 0 \\ m\delta_e & m_{\dot{u}_g}\frac{\bar{c}}{V}\sigma_{\hat{u}_g}\sqrt{\frac{2V}{l_g}} & m_{\dot{\alpha}_g}\frac{\bar{c}}{V}\sigma_{\alpha_g}\sqrt{\frac{3V}{l_g}} \\ 0 & \sigma_{\dot{u}_g}\sqrt{\frac{2V}{L_g}} & 0 \\ 0 & 0 & \sigma_{\alpha_g}\sqrt{\frac{3V}{l_g}} \\ 0 & 0 & (1-2\sqrt{3})\sigma_{\alpha_g}\sqrt{(\frac{V}{L_g})^3} \end{bmatrix} \tag{5}$$

$$A = \begin{bmatrix} -0.0022 & 0.1152 & -0.1561 & 0 & -0.0022 & 0.1152 & 0 \\ -0.3114 & -3.9245 & 0 & 57.7410 & -0.3114 & -3.9245 & 0.0461 \\ 0 & 0 & 0 & 61.0963 & 0 & 0 & 0 \\ 0.0205 & -0.2167 & 0 & -5.2043 & 0.0205 & -0.2167 & 0.0226 \\ 0 & 0 & 0 & 0 & -0.8378 & 0 & 0 \\ 0 & 0 & 0 & 0 & 0 & 0 & 1 \\ 0 & 0 & 0 & 0 & 0 & -0.7020 & -1.6757 \end{bmatrix} \tag{6}$$

$$B = \begin{bmatrix} 0 & 0 & 0 \\ -0.3932 & 0 & 0.0006 \\ 0 & 0 & 0 \\ -0.6435 & 0 & 0.0003 \\ 0 & 0.0103 & 0 \\ 0 & 0 & 0.0126 \\ 0 & 0 & -0.0150 \end{bmatrix} \tag{7}$$

1.2 Controlled Complete Aircraft Model

It is proven that that the symmetric aircraft model is not stable in the applicable flight condition. Therefore, a pitch damper is designed consisting of a feedback matrix K which is shown in equation 8. With this an updated A matrix can be constructed which is done in equation 9. The eigenvalues of this matrix are shown in table 1 and can be inspected visually in the pole-zero map of figure 2. From this it can be observed that with this controller the controlled aircraft model is stable.

$$K = \begin{bmatrix} 0 & 0 & K_t & K_q & 0 & 0 & 0 \end{bmatrix} = \begin{bmatrix} 0 & 0 & -0.21 & 0 & 0 & 0 & 0 \end{bmatrix} \tag{8}$$

$$A_{controlled} = A - BK = \begin{bmatrix} -0.00218 & 0.1152 & -0.1561 & 0 & -0.00218 & 0.1152 & 0 \\ -0.3114 & -3.924 & -0.08257 & 57.74 & -0.3114 & -3.924 & 0.04608 \\ 0 & 0 & 0 & 61.1 & 0 & 0 & 0 \\ 0.0205 & -0.2167 & -0.1351 & -5.204 & 0.0205 & -0.2167 & 0.02263 \\ 0 & 0 & 0 & 0 & -0.8378 & 0 & 0 \\ 0 & 0 & 0 & 0 & 0 & 0 & 1.0 \\ 0 & 0 & 0 & 0 & 0 & -0.702 & -1.676 \end{bmatrix} \tag{9}$$

1.3 Reduced Aircraft Model

From the complete model a reduced aircraft model can be constructed. This is done based on the assumptions applicable to the short-period motion. During the short period it can be assumed that the airspeed remains constant and that the trajectory of the centre of gravity moves along a horizontal straight line. This means that the flight path angle γ will always be equal to zero. Because of this $\hat{u}$ and θ can be omitted from the state which results in the system given by equation 10. The reduced A and B matrices are shown in equations 11 and 12. Substituting the constants of the Cessna Ce550 Citation II gives the reduced matrices depicted by equations 13 and 14. The eigenvalues of this matrix are shown in table 1 and can be inspected visually in the pole-zero map of figure 3. From this it can be observed that the reduced symmetric aircraft model is stable in the applicable flight condition.

$$X = \begin{bmatrix} \alpha & \frac{q\bar{c}}{V} & \hat{u}_g & \alpha_g & \alpha_g^* \end{bmatrix}^T \tag{10}$$

$$A_{reduced} = \begin{bmatrix} z_\alpha & z_q & z_{u_g} - z_{\dot{u}_g}\frac{V}{L_g}\frac{\bar{c}}{V} & z_{\alpha_g} & z_{\dot{\alpha}_g}\frac{\bar{c}}{V} \\ M_\alpha & m_q & m_{u_g} - m_{\dot{u}_g}\frac{V}{L_g}\frac{\bar{c}}{V} & m_{\alpha_g} & m_{\dot{\alpha}_g}\frac{\bar{c}}{V} \\ 0 & 0 & -\frac{V}{L_g} & 0 & 0 \\ 0 & 0 & 0 & 0 & 1 \\ 0 & 0 & 0 & -\frac{V^2}{L_g^2} & -2\frac{V}{L_g} \end{bmatrix} \tag{11}$$

$$B_{reduced} = \begin{bmatrix} z_{\delta_e} & z_{\dot{u}_g}\frac{\bar{c}}{V}\sigma_{\hat{u}_g}\sqrt{\frac{2V}{l_g}} & z_{\dot{\alpha}_g}\frac{\bar{c}}{V}\sigma_{\alpha_g}\sqrt{\frac{3V}{l_g}} \\ m\delta_e & m_{\dot{u}_g}\frac{\bar{c}}{V}\sigma_{\hat{u}_g}\sqrt{\frac{2V}{l_g}} & m_{\dot{\alpha}_g}\frac{\bar{c}}{V}\sigma_{\alpha_g}\sqrt{\frac{3V}{l_g}} \\ 0 & \sigma_{\dot{u}_g}\sqrt{\frac{2V}{L_g}} & 0 \\ 0 & 0 & \sigma_{\alpha_g}\sqrt{\frac{3V}{l_g}} \\ 0 & 0 & (1-2\sqrt{3})\sigma_{\alpha_g}\sqrt{(\frac{V}{L_g})^3} \end{bmatrix} \tag{12}$$

$$A_{reduced} = \begin{bmatrix} -3.924 & 57.74 & -0.3114 & -3.924 & 0.04608 \\ -0.2167 & -5.204 & 0.0205 & -0.2167 & 0.02263 \\ 0 & 0 & -0.8378 & 0 & 0 \\ 0 & 0 & 0 & 0 & 1.0 \\ 0 & 0 & 0 & -0.702 & -1.676 \end{bmatrix} \tag{13}$$

$$\begin{bmatrix} -0.3932 & 0 & 0.0005813 \\ -0.6435 & 0 & 0.0002855 \\ 0 & 0.0103 & 0 \\ 0 & 0 & 0.01262 \\ 0 & 0 & -0.01504 \end{bmatrix} \tag{14}$$

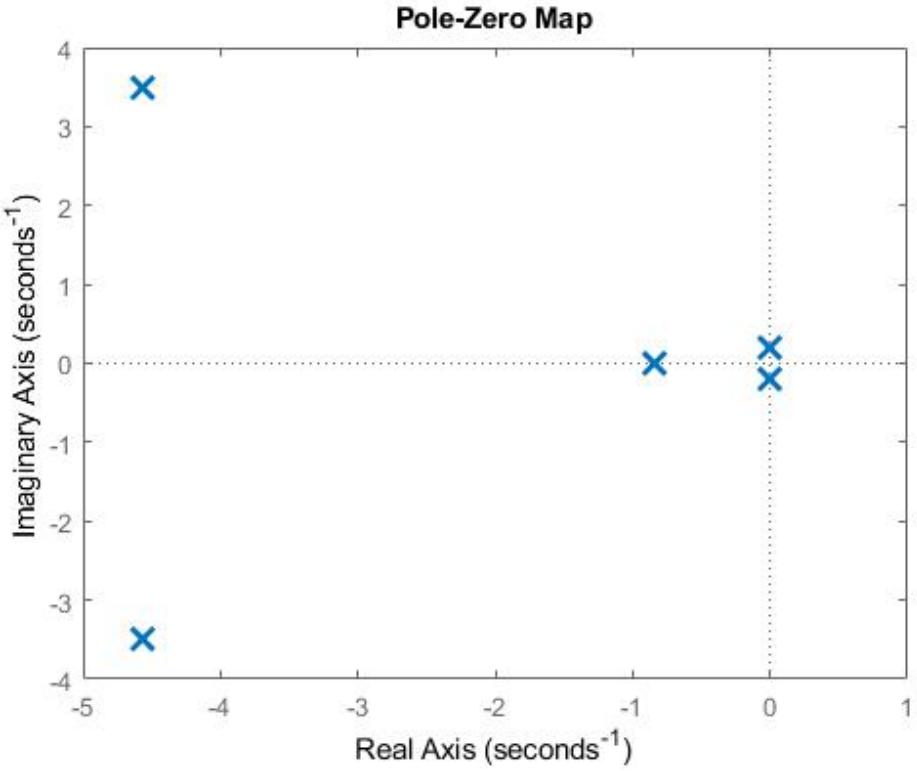

Figure 1: Pole locations for the uncontrolled systems

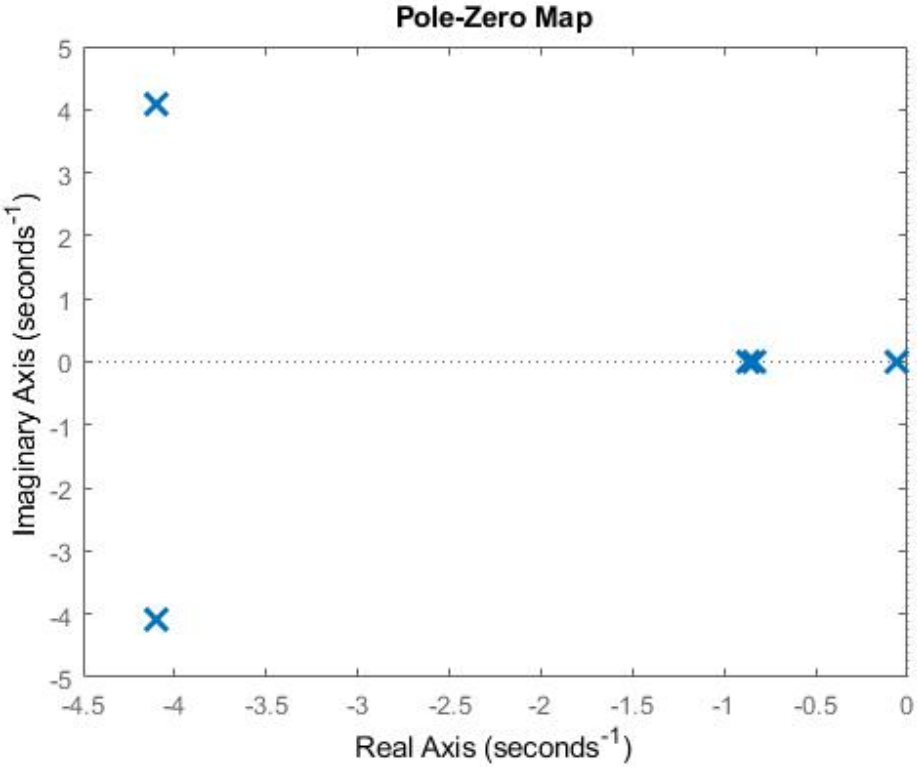

Figure 2: Pole locations for the controlled systems

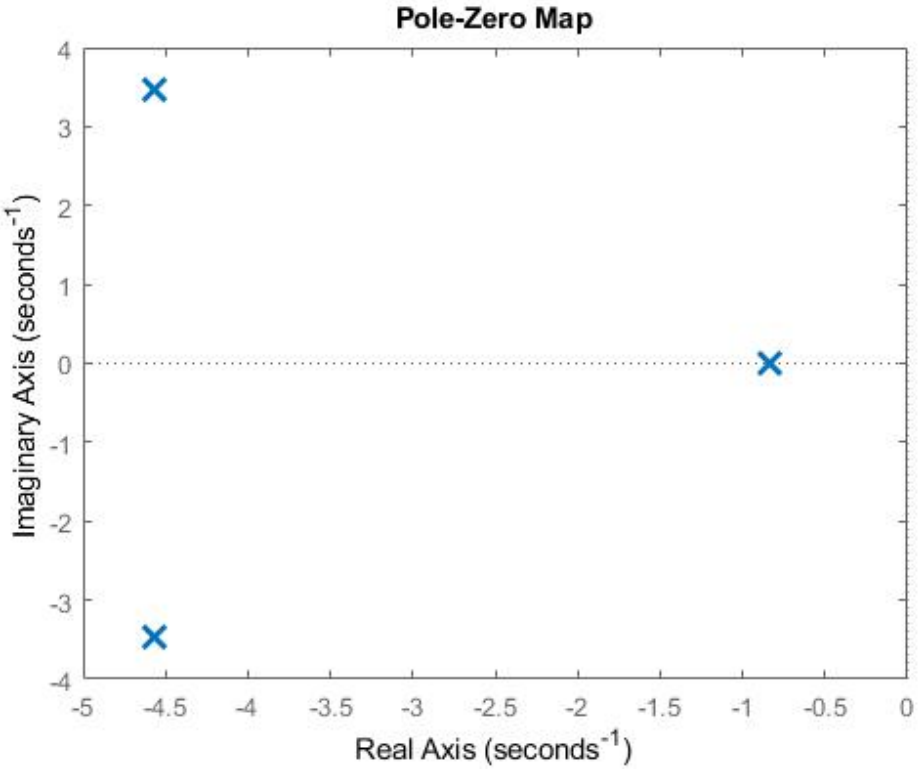

Figure 3: Pole locations for the reduced systems

Uncontrolled system	**Controlled system**	**Reduced system**
-4.5666 + 3.4811i	-4.1007 + 4.0937i	-4.5644 + 3.4792i
-4.5666 - 3.4811i	-4.1007 - 4.0937i	-4.5644 - 3.4792i
0.0011 + 0.2069i	-0.0613	-0.8378
0.0011 - 0.2069i	-0.8682	-0.8378
-0.8378	-0.8378	-0.8378
-0.8378	-0.8378	
-0.8378	-0.8378	

Table 1: Eigenvalues of the uncontrolled, controlled and reduced model

2 Time-Domain Analysis

In this section, a time-domain analyses will be performed on the complete and the reduced aircraft model for all aircraft states and the load factor. In both models Matlab's Randn.m function is used to simulate the longitudinal and vertical turbulence. To obtain the time responses, the C and D matrices need to be constructed such that the desired states are an output of the system. The load factor is defined by equation 15 and will be implemented in the C and D matrices of the complete aircraft model as shown in equation 16 and 17. The outputs computed are velocity deviation $\hat{u}$, angle of attack α, pitch angle θ, pitch rate $\frac{q\bar{c}}{V}$ and the load factor n_z. Substituting the constants of the Cessna Ce550 Citation II gives the matrices depicted by equations 18 and 19. The time responses of the system are shown in figures 4-8.

$$n_z = \frac{a_z}{g} = \frac{1}{g}\frac{d^2h}{dt^2} = \frac{1}{g}\frac{d}{dt}Vsin\gamma \approx \frac{V}{g}\dot{\gamma} = \frac{V}{g}(\dot{\theta} - \dot{\alpha}) \tag{15}$$

$$C_{complete} = \begin{bmatrix} 1 & 0 & 0 & 0 & 0 & 0 & 0 \\ 0 & 1 & 0 & 0 & 0 & 0 & 0 \\ 0 & 0 & 1 & 0 & 0 & 0 & 0 \\ 0 & 0 & 0 & 1 & 0 & 0 & 0 \\ -\frac{V}{g}z_u & -\frac{V}{g}z_\alpha & -\frac{V}{g}z_\theta & \frac{V}{g}(\frac{V}{\bar{c}} - z_q) & -\frac{V}{g}(z_{u_g} - z_{\dot{u}_g}\frac{V}{L_g}\frac{\bar{c}}{V}) & -\frac{V}{g}z_{\alpha_g} & -\frac{V}{g}z_{\dot{\alpha}_g}\frac{\bar{c}}{V} \end{bmatrix} \tag{16}$$

$$D_{complete} = \begin{bmatrix} 0 & 0 & 0 \\ 0 & 0 & 0 \\ 0 & 0 & 0 \\ 0 & 0 & 0 \\ -\frac{V}{g}z_{\delta_e} & -\frac{V}{g}z_{\dot{u}_g}\frac{\bar{c}}{V}\sigma_{\hat{u}_g}\sqrt{\frac{2V}{l_g}} & -\frac{V}{g}z_{\dot{\alpha}_g}\frac{\bar{c}}{V}\sigma_{\alpha_g}\sqrt{\frac{3V}{l_g}} \end{bmatrix} \tag{17}$$

$$C_{complete} = \begin{bmatrix} 1 & 0 & 0 & 0 & 0 & 0 & 0 \\ 0 & 1 & 0 & 0 & 0 & 0 & 0 \\ 0 & 0 & 1 & 0 & 0 & 0 & 0 \\ 0 & 0 & 0 & 1 & 0 & 0 & 0 \\ 3.9905 & 50.2934 & 1.0581 & 42.9980 & 3.9905 & 50.2934 & -0.5906 \end{bmatrix} \tag{18}$$

$$D_{complete} = \begin{bmatrix} 0 & 0 & 0 \\ 0 & 0 & 0 \\ 0 & 0 & 0 \\ 0 & 0 & 0 \\ 5.0386 & 0 & -0.0074 \end{bmatrix} \tag{19}$$

For the reduced aircraft model the states are the angle of attack α and the pitch rate $\frac{q\bar{c}}{V}$. In the reduced model the pitch rate is equal to the angle of attack due to the assumption that the trajectory of the centre of gravity moves along a horizontal straight line. Therefore, the load factor will always be zero for the reduced aircraft model and will not be added to the time-domain analysis results. The C and D matrices are constructed to obtain the two desired outputs and are shown in equation 20. The time responses of the system are shown in figures 9 and 10.

$$C_{reduced} = \begin{bmatrix} 1 & 0 & 0 & 0 & 0 \\ 0 & 1 & 0 & 0 & 0 \end{bmatrix} D_{reduced} = \begin{bmatrix} 0 & 0 & 0 \\ 0 & 0 & 0 \end{bmatrix} \tag{20}$$

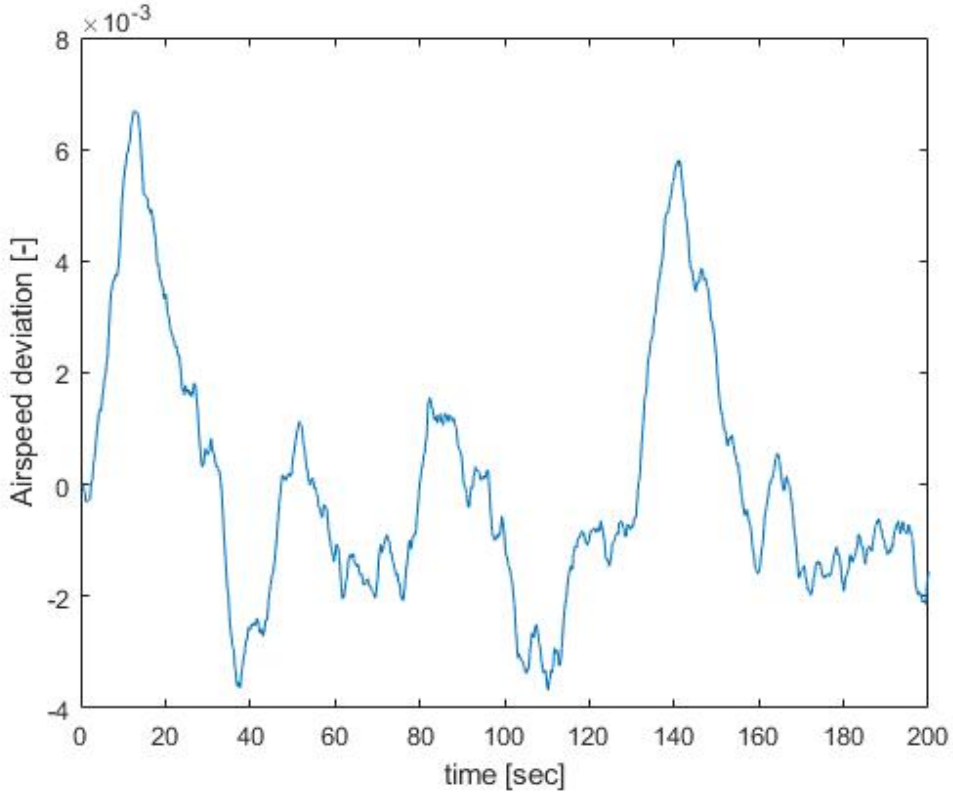

Figure 4: Airspeed deviation time response for the complete model

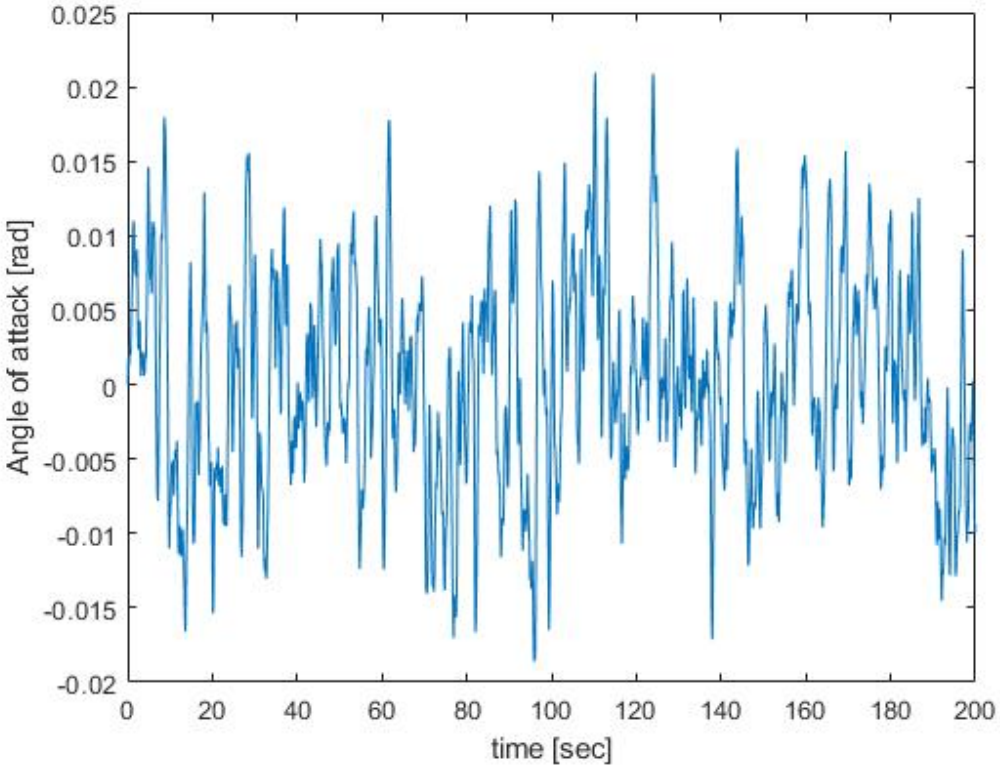

Figure 5: Angle of attack time response for the complete model

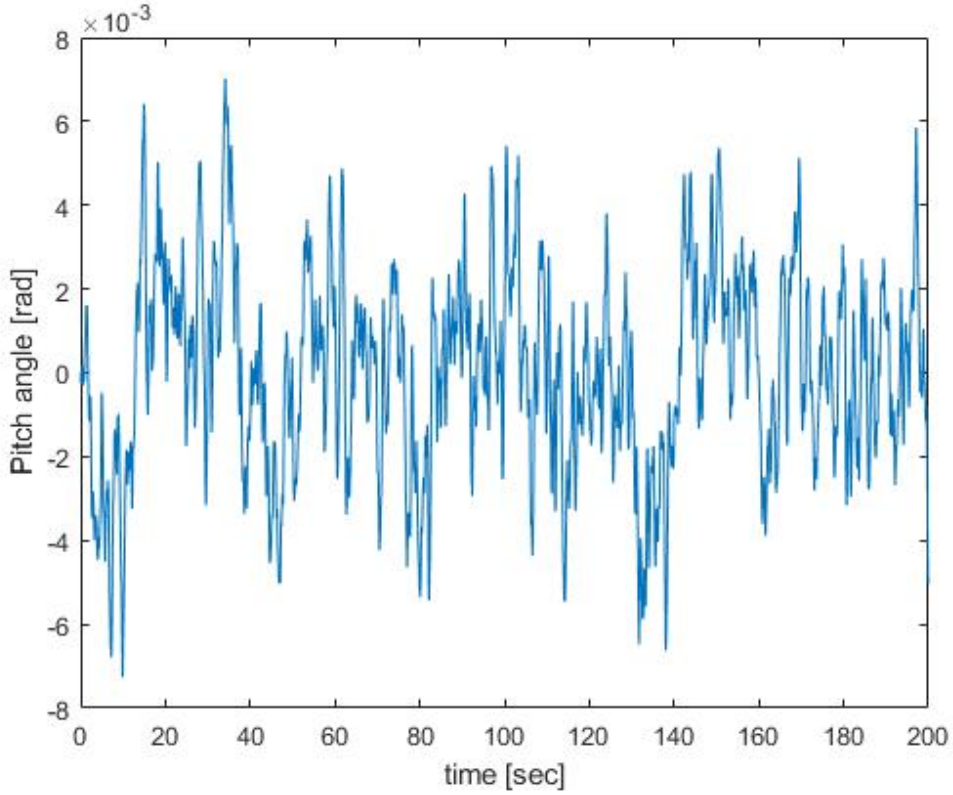

Figure 6: Pitch angle time response for the complete model

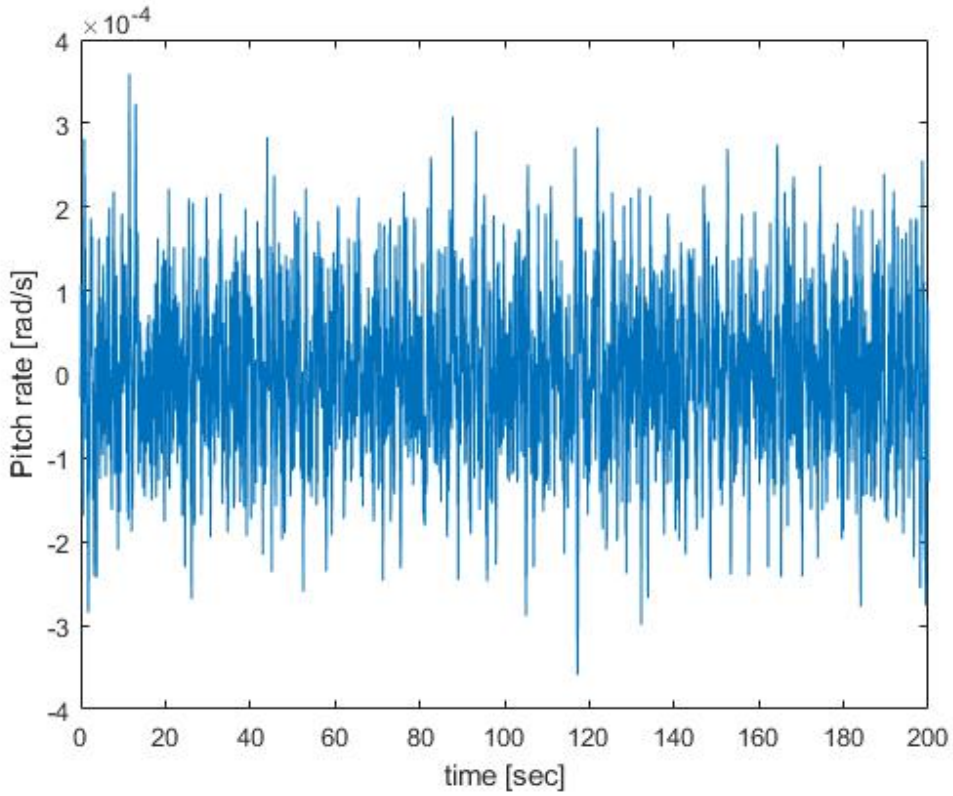

Figure 7: Pitch rate time response for the complete model

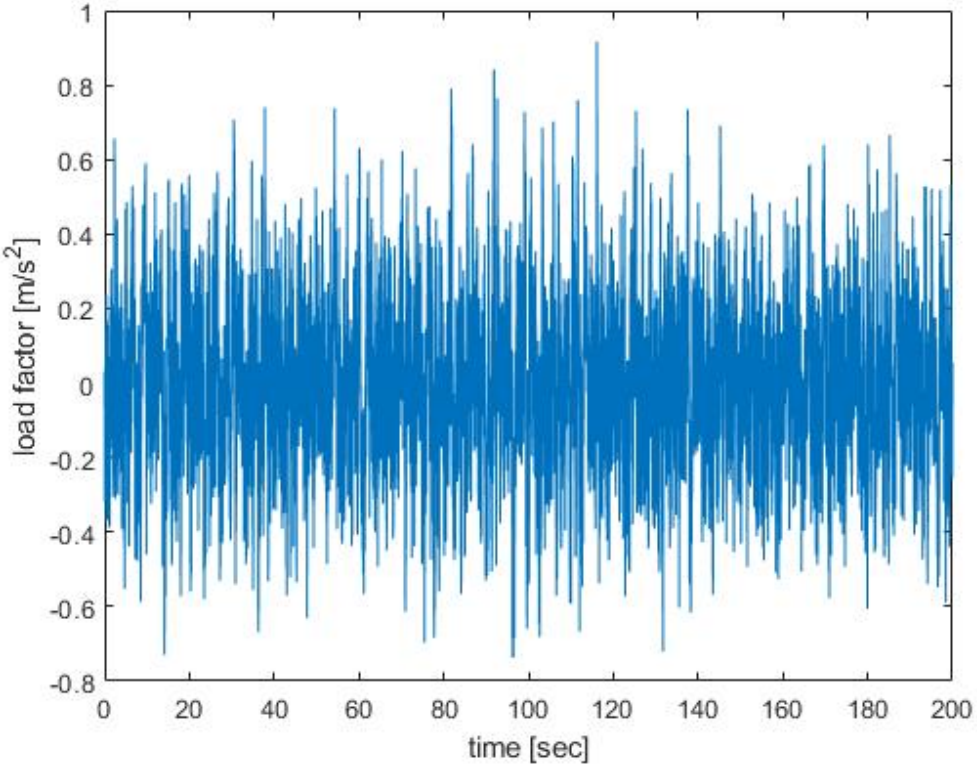

Figure 8: Load factor time response for the complete model

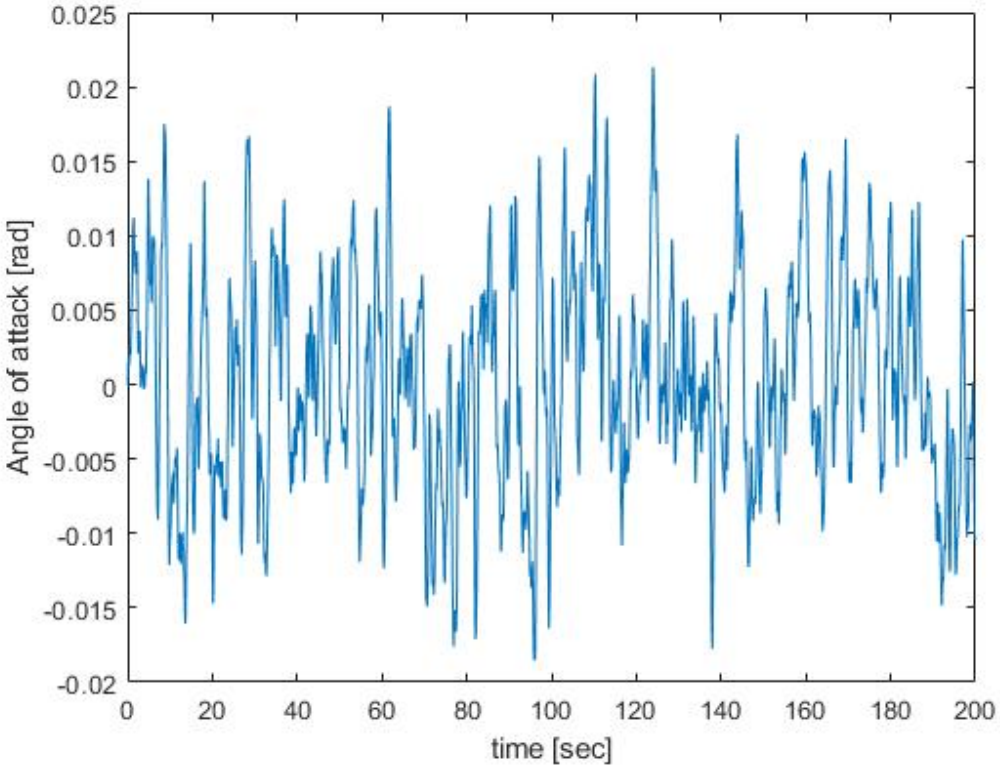

Figure 9: Angle of attack time response for the reduced model

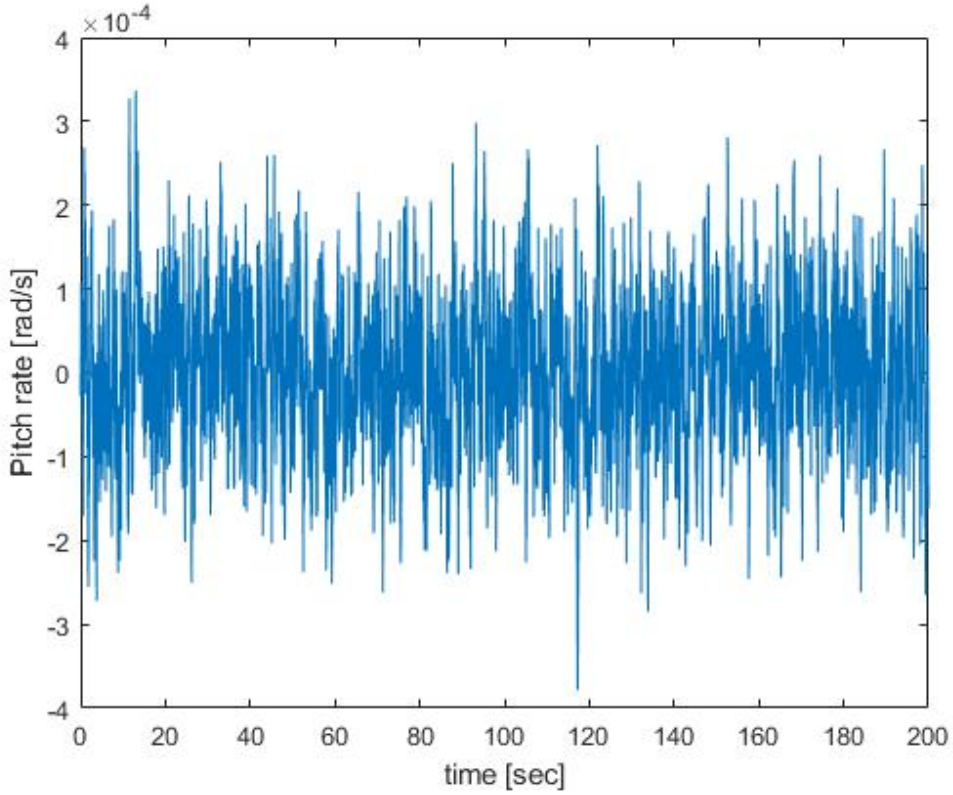

Figure 10: Pich rate time response for the reduced model

3 Spectral Analysis

In this section, the Power Spectral density will be calculated for all the aircraft states and the load factor using both models. The Power Spectral Density refers to signal power as a function of frequency and will be calculated by three different methods. After this, a brief discussion will be done where the differences between the aircraft models will be explained. Finally, the differences found between the calculation methods of the periodograms is explained. The Power Spectral Densities of all aircraft states and the load factor are shown in the figures 11-16.

3.1 Calculation methods

The Power Spectral Density functions are estimated analytically using the state space representation, experimentally using the Matlab routine fft.m and smoothed experimentally:

- **Analytic:**
  In order to calculate the analytic Power Spectral Density the bode plot magnitude is used which can be constructed with Matlab's bode.m command. The analytical expression of the Power Spectral Density is given by equation 21 where G(ω) represents the frequency response.

$$S_w = \lim_{T\to\infty} \frac{1}{2T}|G(w)|^2 \tag{21}$$

- **Experimental:**
  To obtain the experimental Power Spectral Densities the Fast Fourier Transform (FFT) is applied on the time responses. The FFT algorithm is based on the divide and conquer algorithm and is therefore a fast method to compute the DFT. The DFT is computed in equation 22 and is used to obtain the DFT of the individual signals in in equation 23. By summing these components the DFT of the original signal is obtained.

$$\bar{X}[k] = \sum_{n=0}^{N-1} \hat{x}[n]e^{-jk\frac{2\pi}{N}n} \tag{22}$$

$$I_{N_{xx}}[k] = \frac{|\bar{X}[k]|^2}{N} \tag{23}$$

- **Smoothed experimental:**
  For the smoothed experimental a smoothing function is applied on the experimental Power Spectral Densities. The smoothing function is given in equation 24 where $\Phi[k]$ denotes the the Power Spectral Density obtained at the k^{th} iteration. The first and last entries of the filter output, k=1 and k=N respectively, are defined as equal to the unsmoothed Power Spectral Density.

$$\Phi_{estimate}[k] = 0.25\Phi[k-1] + 0.5\Phi[k] + 0.25\Phi[k+1] \tag{24}$$

3.2 Differences between aircraft models

In this subsection, the difference found between the different aircraft models will be explained for the angle of attack α and the pitch rate $\frac{q\bar{c}}{V}$. From figures 12 and 13 it can be seen that no noticeable differences are present in Power Spectral Densities of both aircraft models related to the angle of attack. In contrast to this, the Power Spectral Densities related to the pitch rates does show some noticeable differences as shown in figures 15 and 16. It can bee seen that the slope at lower frequencies is higher for the controlled system compared to the reduced system.

3.3 Differences between calculation methods

As can be observed from the figures 11-16 that the analytical Power Spectral Densities are more straight and continuous. This is due to the fact that all the inputs are deterministic which makes the analytical Power Spectral Density impractical in real life. The experimental Power Spectral Density however, is computed using the time responses due to a stochastic input. This is done to simulate white noise and it can be seen that this causes the Power Spectral Densities to be unsmooth with steep peaks. These peaks can be filtered using the smoothed function which calculates the weighted mean value of the $k-1^{th}$, the k^{th} and the $k+1^{th}$ iteration. As it can be seen in the figures this makes the experimental Power Spectral Density more smooth. Also, when observing the velocity deviation $\hat{u}$ it can be seen that experimental Power Spectral Density deviates from the analytical Power Spectral Density at higher frequencies. This is caused by spectral leakage which occurs when the signal does not fit an integer number of times inside the measured time.

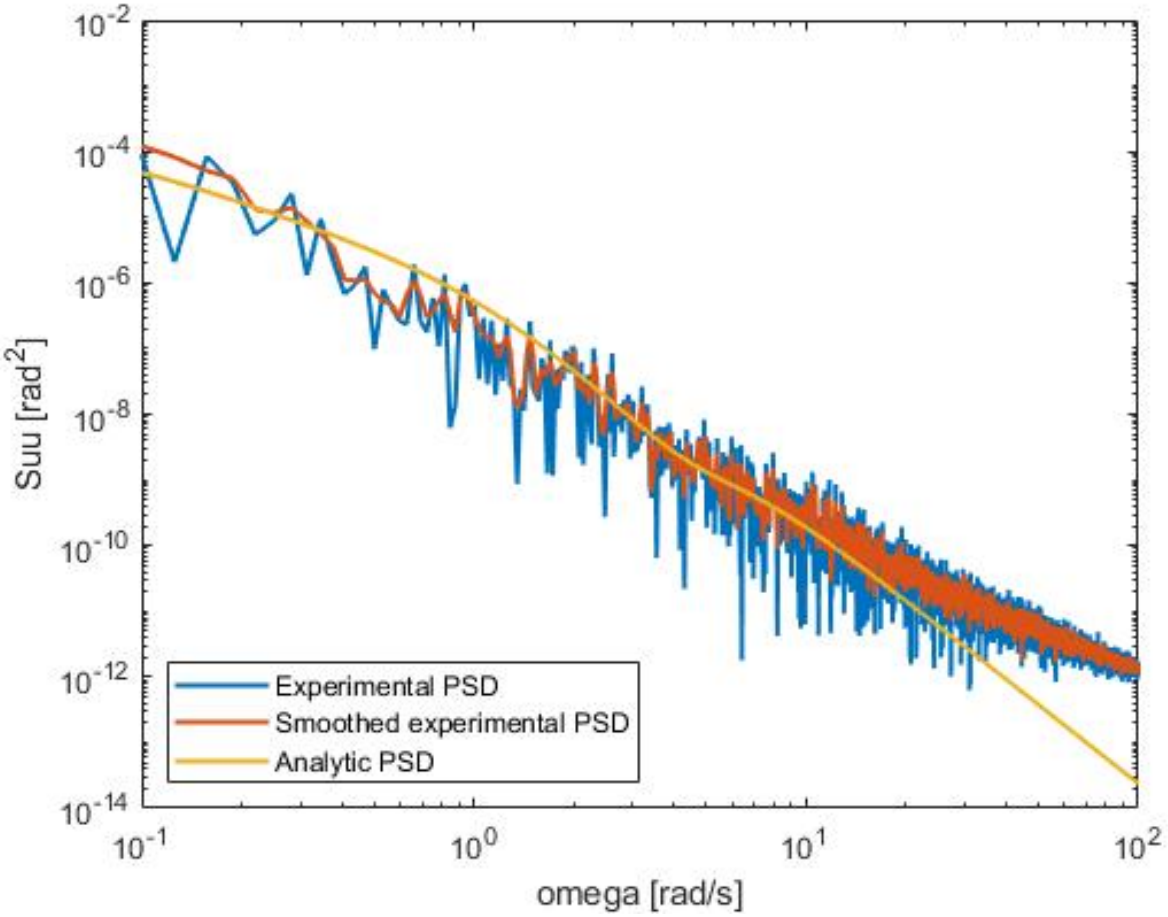

Figure 11: Power spectral density of the velocity for the complete system

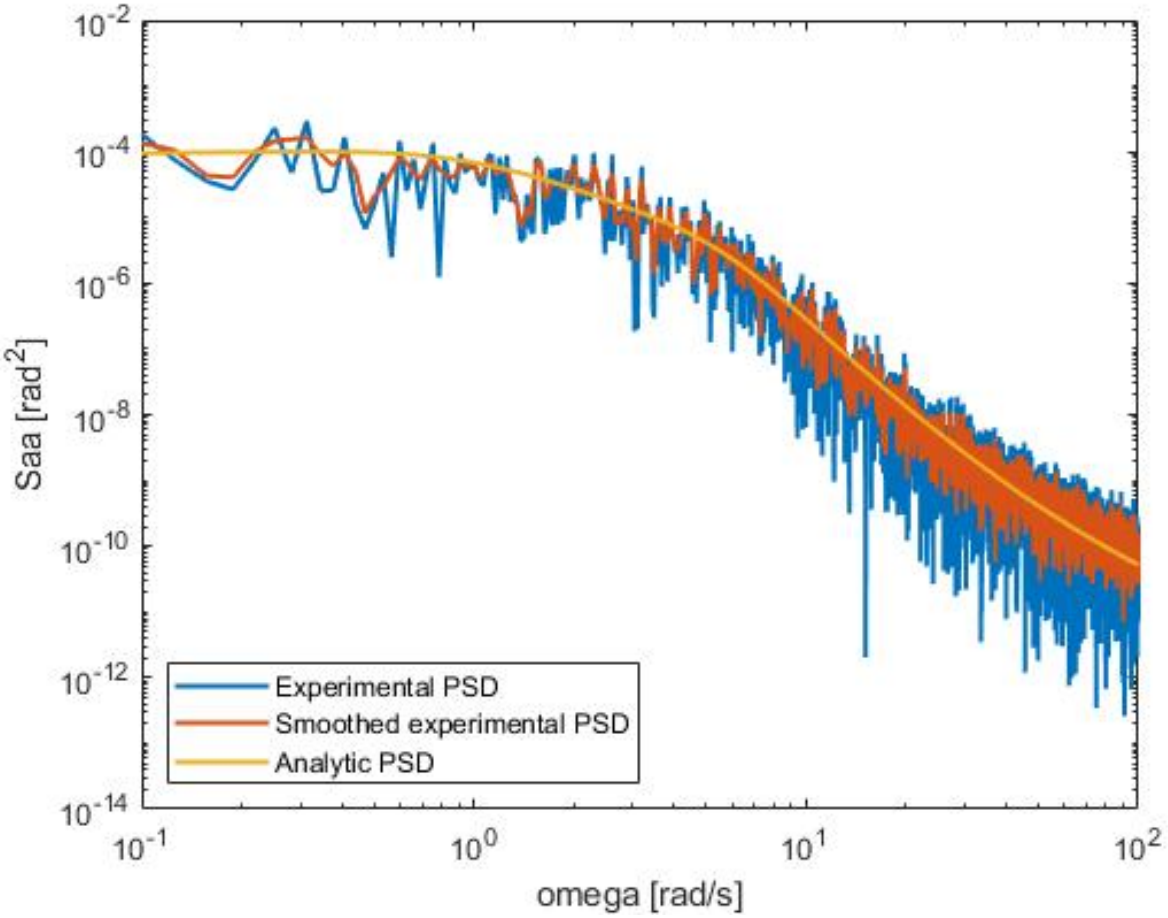

Figure 12: Power spectral density of the angle of attach for the complete system

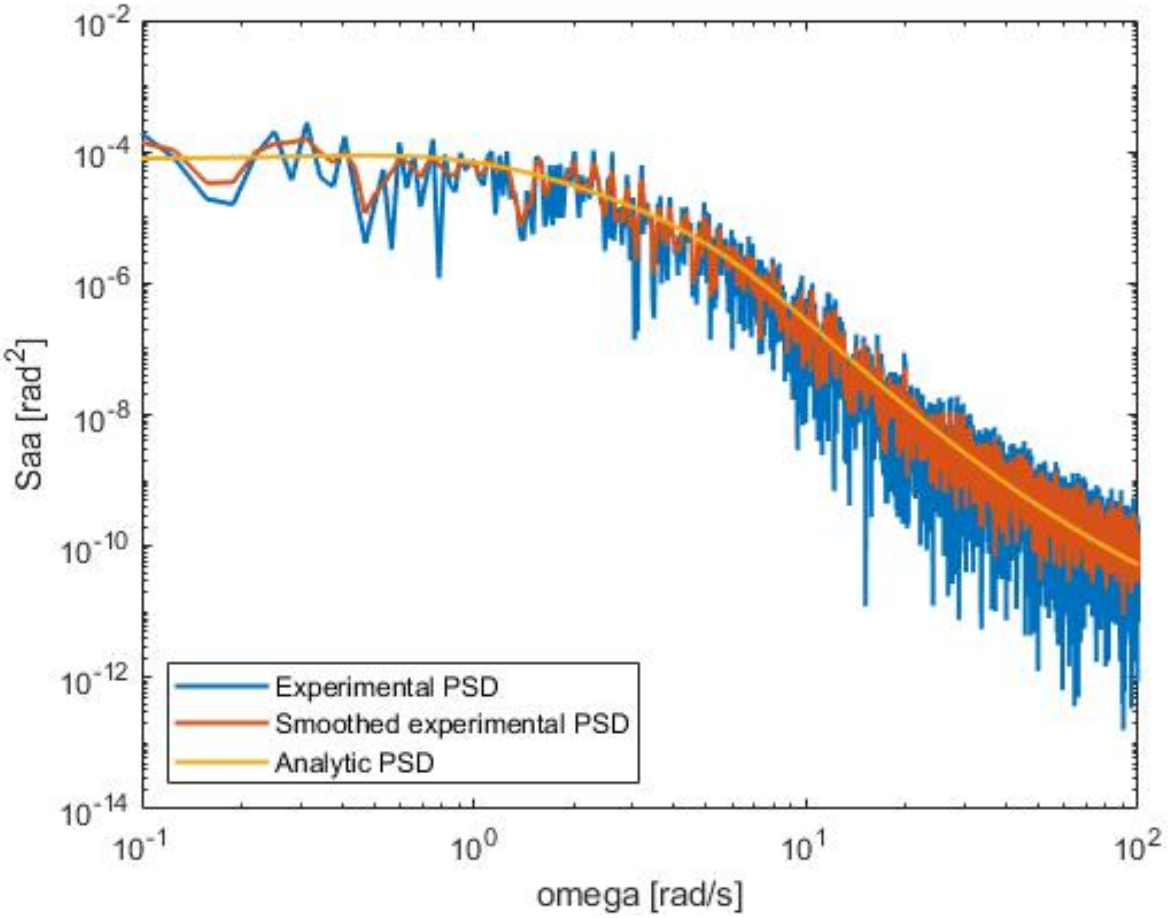

Figure 13: Power spectral density of the angle of attack for the reduced system

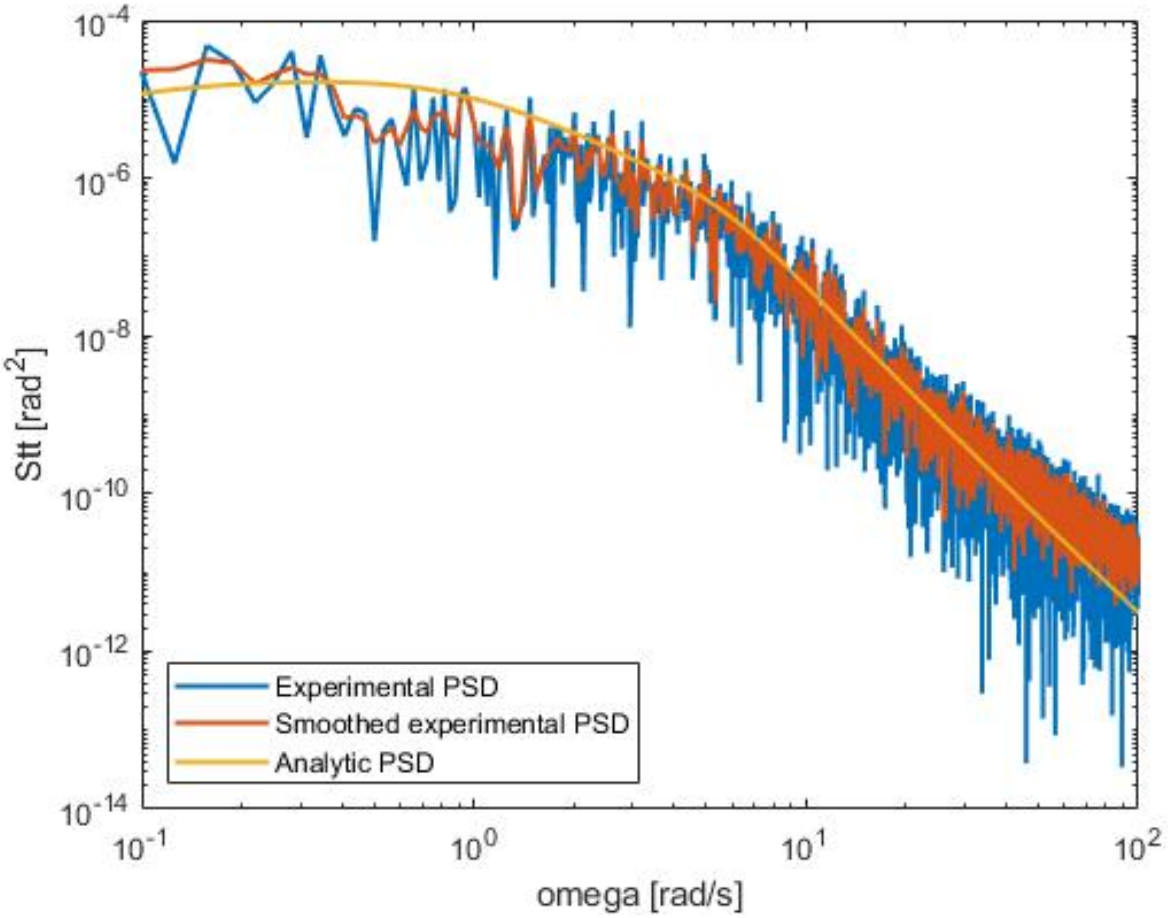

Figure 14: Power spectral density of the pitch angle for the complete system

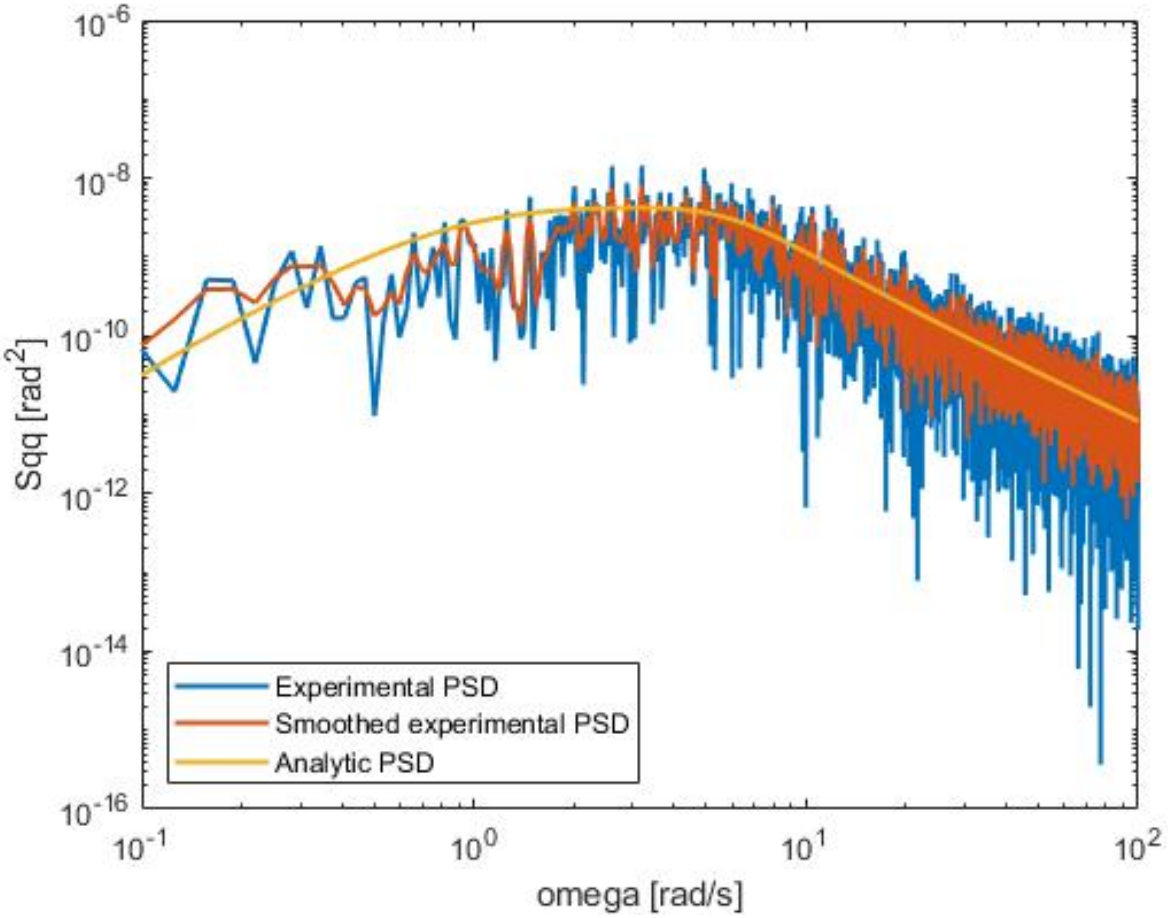

Figure 15: Power spectral density of the pitch rate for the complete system

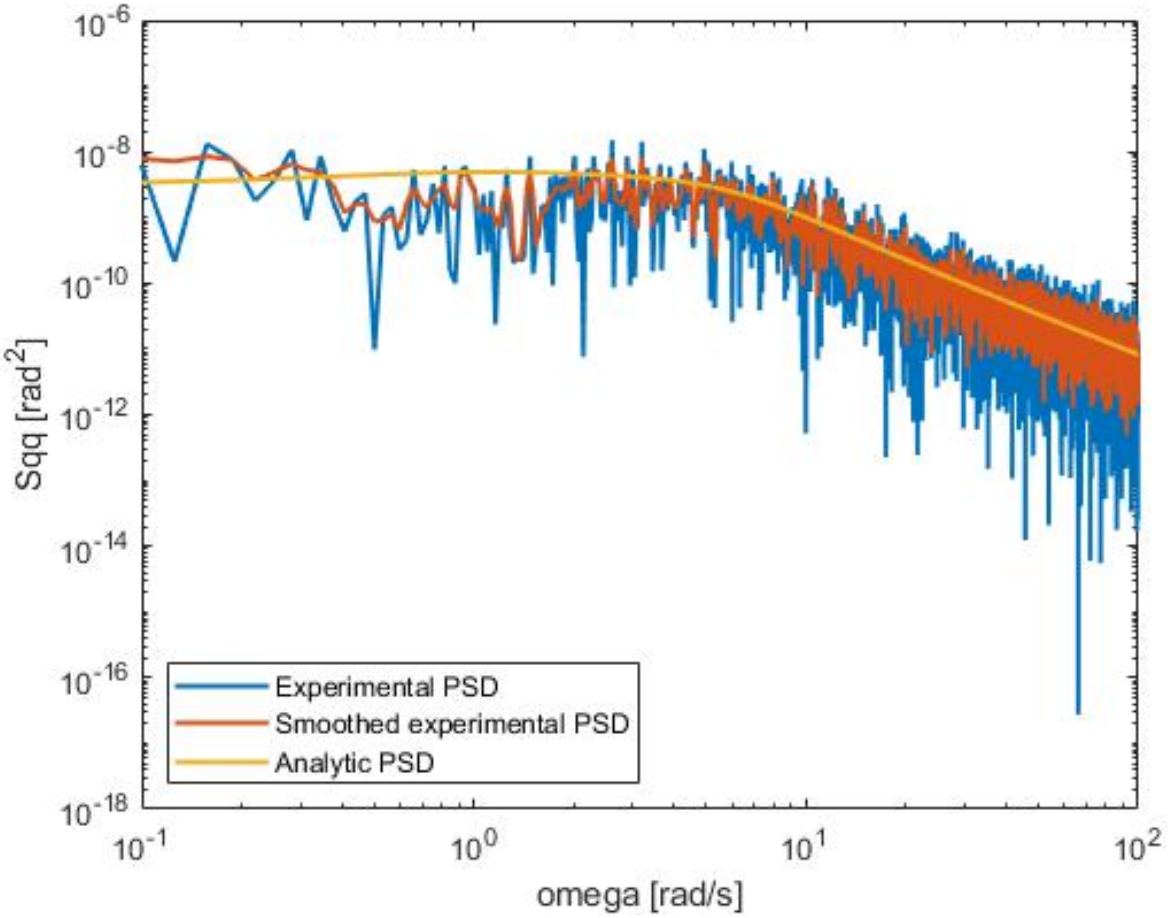

Figure 16: Power spectral density of the pitch rate for the reduced system

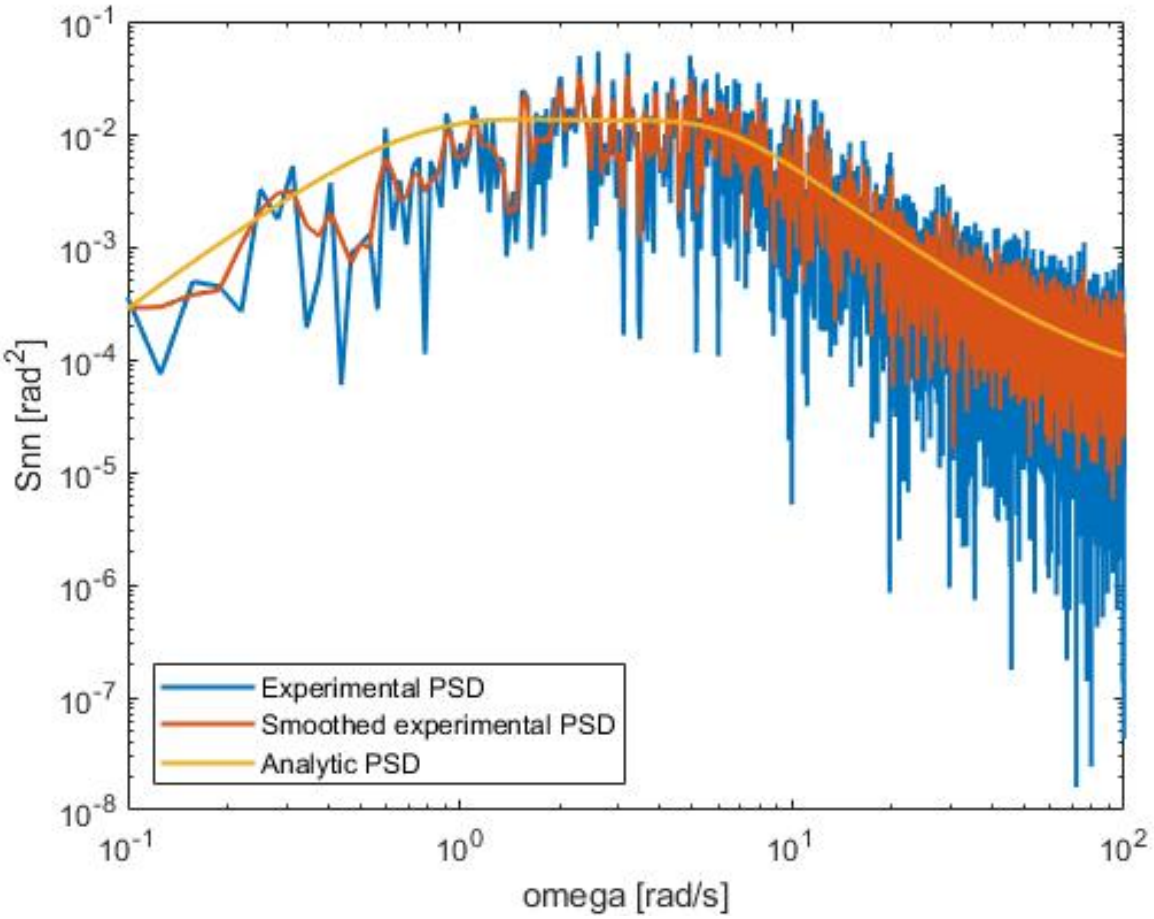

Figure 17: Power spectral density of the load factor for the complete system

4 Variances

In this section, the variances of all aircraft states and the load factor will be estimated. The variance is the expectation of the squared deviation of a random variable from its mean and will be calculated using three different methods. After this, a brief discussion will be done where the differences between the aircraft models will be explained. Finally, the differences found between the variance calculation methods will be explained. The calculated variances of all aircraft states and the load factor for the complete and reduced model are shown in table 2 and 3 respectively.

4.1 Calculation methods

The variances are estimated using the analytical power spectra, the Impulse Response method and the Matlab routine var.m:

- **Analytical:**
  For the calculation of the variance using the analytical power spectra the formula given in equation 25 is used where $S(\omega)$ denotes the analytical Power Spectral density calculated in the previous section. This method is also known as crude integration of spectral densities which could also be done for the experimental Power Spectral Densities.

$$\sigma^2 = \frac{1}{\pi}\int_0^\infty S(\omega)d\omega \tag{25}$$

- **Impulse Response:**
  The Impulse Response method uses the relation shown in equation 26 to calculate the variance. It is proven that a response to an initial condition ($x(0) = B_i$) is identical to an impulse response. By integrating the product of the impulse responses, the growth in time of the covariance matrix can be calculated.

$$\sigma_{\bar{x}}^2 = C_{\bar{x}\bar{x}}(0) \tag{26}$$

- **Matlab routine var.m:**
  The Matlab function var.m calculates the variance using the formula given in equation 27. In this equation μ_x is denoted as the mean of the data set and X_i denotes the current value.

$$\sigma^2 = \frac{1}{N-1}\sum_{i=1}^{N}|X_i - \mu_x| \tag{27}$$

4.2 Differences between aircraft models

Similar to the Power Spectral Density there exist a subtle difference between the aircraft models. As the variance basically can be estimated by the area under the Power Spectral Density function we observe a similar difference as in the previous section. The variances calculated related to the angle of attack α are more similar compared to the pitch rate $\frac{q\bar{c}}{V}$. Because the Power Spectral Density of the complete aircraft model has a lower value in the lower frequencies it has more area and therefore a higher variance. This behavior can be observed for all calculation methods.

4.3 Differences between calculation methods

As the analytical Power Spectral Density is constructed from deterministic variables it shows differences with the other methods which are determined using the stochastic time responses. This is due to the fact that the time responses are taken with a duration of just 200 seconds. When the time response is taken over an infinite interval the differences should become zero. This behavior can be observed in tables 2 and 3 where it can be seen that the analytical power spectra method gives a higher variance.

State	Analytical power spectra	Impulse response method	MATLAB routine var.m
$\hat{u}$ $[rad^2]$	4.617e-06	2.962e-06	2.927e-06
α $[rad^2]$	5.632e-05	5.024e-05	4.980e-05
θ $[rad^2]$	8.081e-06	3.741e-06	3.706e-06
$\frac{q\bar{c}}{V}$ $[rad^2]$	1.192e-08	7.773e-09	7.702e-09
n_z $[m^2/s^4]$	0.06578	0.04183	0.04138

Table 2: Variances calculated for the controlled model

State	Analytical power spectra	Impulse response method	MATLAB routine var.m
α $[rad^2]$	5.517e-05	4.208e-05	4.177e-05
$\frac{q\bar{c}}{V}$ $[rad^2]$	1.247e-08	8.461e-09	8.418e-09

Table 3: Variances calculated for the reduced model

5 Conclusion

In this report, the symmetrical aircraft responses for a rigid Cessna Ce550 Citation II in cruise configuration subjected to symmetrical atmospheric turbulence is analysed. In the first section, the complete and the reduced aircraft model, from which the latter one is based on the assumptions for the short-period, are defined. In contrary to the reduced aircraft model, the complete aircraft model is proven to be unstable and therefore a pitcher-damper is designed.

After this, the time-domain simulation results of the aircraft states are shown for the complete and the reduced aircraft model. The states simulated for the complete model are the airspeed deviation $\hat{u}$, the angle of attack α, the pitch angle θ, the pitch rate $\frac{q\bar{c}}{V}$ and the load factor n_z. For the reduced aircraft model only the angle of attack α and the pitch rate $\frac{q\bar{c}}{V}$ are simulated.

Next, a spectral analysis is conducted by calculating the Power Spectral Densities of all the states mentioned above using three different methods. The Power Spectral Densities are first calculated analytically after which they are calculated experimentally to apply a smoothing filter on the experimental Power Spectral Densities at last. The Power Spectral Density of the pitch rate in the reduced model shows a higher slope in the lower frequency compared to the complete model. Furthermore, it can be observed that the analytical Power Spectral Densities are more straight compared to the (smoothed) experimental Power Spectral Densities due to the deterministic input. At last, the Power Spectral Densities of the airspeed deviation show differences in the higher frequencies due to leakage.

At last, the variances of all states mentioned above for both aircraft models are estimated. This is done using the analytical power spectra, the impulse response method and using the Matlab routine var.m. Due to the fact that, the Power Spectral Density of the pitch rate in the reduced aircraft model has a higher slope in the lower frequencies, the variances of the pitch rate in the reduced model are lower. Also, it can be observed that the the analytical power spectra is higher compared to the other calculation methods. This is due to the fact that the time simulations are measured for a finite time.